Horizontal-Disparity Tuning of Neurons in the Visual Forebrain of the Behaving Barn Owl

ANDREAS NIEDER AND HERMANN WAGNER
Lehrstuhl für Zoologie/Tierphysiologie, Institut für Biologie II, Rheinisch-Westfälische Technische Hochschule Aachen, D-52074 Aachen, Germany

Nieder, Andreas and Hermann Wagner. Horizontal-disparity tuning of neurons in the visual forebrain of the behaving barn owl. *J. Neurophysiol.* 83: 2967–2979, 2000. Stereovision plays a major role in depth perception of animals having frontally-oriented eyes, most notably primates, cats, and owls. Neuronal mechanisms of disparity sensitivity have only been investigated in anesthetized owls so far. In the current study, responses of 160 visual Wulst neurons to static random-dot stereograms (RDS) were recorded via radiotelemetry in awake, fixating barn owls. The majority of neurons (76%) discharged significantly as a function of horizontal disparity in RDS. The distribution of preferred disparities mirrored the behaviorally relevant range of horizontal disparities that owls can exploit for depth vision. Most tuning profiles displayed periodic modulation and could well be fitted with a Gabor function as expected if disparity detectors were implemented according to the disparity energy model. Corresponding to this observation, a continuum of tuning profiles was observed rather than discrete categories. To assess a possible clustering of neurons with similar disparity-tuning properties, single units, and multi-unit activity recorded at individual recording sites were compared. Only a minority of neurons were clustered according to their disparity-tuning properties, suggesting that neurons in the visual Wulst are not organized into columns by preferred disparity. To assess whether variable vergence eye movements influenced tuning data, we correlated tuning peak positions on a trial-by-trial basis for units that were recorded simultaneously. The general lack of significant correlation between single-trial peak positions of simultaneously recorded units indicated that vergence, if at all, had only a minor influence on the data. Our study emphasizes the significance of visual Wulst neurons in analyzing stereoscopic depth information and introduces the barn owl as a second model system to study stereopsis in awake, behaving animals.

INTRODUCTION

Two slightly displaced images of the visual world are present in the left and right eyes in binocular vision. Stereoscopic depth perception (stereopsis) is based on the visual system's ability to exploit these differences between the two monocular images. Recent behavioral tests demonstrated that barn owls, like monkeys (Bough 1970), possess global stereopsis comparable to that of humans (van der Willigen et al. 1998).

Despite similarities in the perceptual capability to extract depth from horizontal disparity, it is assumed that binocular vision has evolved independently at least twice among the vertebrates, in both mammals and birds (Pettigrew 1986). This independent evolution is manifested by striking differences between the avian and mammalian binocular visual system, raising the question of multiple neural solutions in stereovision. One of the most substantial differences between owls and mammals concerns eye movements. Although mammalian eyes are usually highly movable, eye movements are found in the range of only one or two degrees in owls (Knudsen 1982; Pettigrew and Konishi 1976; Steinbach and Money 1973) and the tubular-shaped eyes fit tightly in the skull (Knudsen 1989). Such a restricted range of eye movements is certainly not useful for gaze orientation, but it is unclear whether they play a role in vergence movements.

The second major difference between owls and mammals is related to the visual pathway. Owls display a total decussation of retinal fibers followed by a partial recrossing of thalamic fibers projecting to the forebrain (Karten et al. 1973). Nevertheless, the physiological properties of the owl's visual forebrain, the visual Wulst, were found to mirror remarkably those of the early stages of mammalian visual cortex. In particular, Wulst neurons display a precise visuotopy, a high degree of binocular interaction, selectivity for orientation and motion direction (Pettigrew and Konishi 1976), and respond even readily to illusory contours (Nieder and Wagner 1999). Furthermore, many disparity-sensitive neurons have been observed in this brain area (Pettigrew 1979; Pettigrew and Konishi 1976). On the basis of preliminary data from the anesthetized owl, Wagner and Frost (1994) suggested that an orderly representation of disparity may be present in the visual Wulst.

Studies on disparity coding in owls have only been performed in anesthetized birds so far, using relatively simple stimuli (bars, gratings, one-dimensional noise) (Pettigrew 1979; Pettigrew and Konishi 1976; Wagner and Frost 1993, 1994). Although these pioneering studies established a neural substrate for avian stereopsis, a closer relationship between activity of disparity-sensitive neurons and depth vision can only be obtained in behaving birds. In the current study, a new approach is presented to study single-cell activity in awake barn owls trained to perform a fixation task. To address representation of global stereopsis, random-dot stereograms (RDS) were applied in which monocular depth cues are abolished and the visual system has to analyze the scene in a wider context (Julesz 1960, 1971). Disparity-tuning curves measured in fixating animals revealed that owls are obviously able to adjust their visual system to a given reference plane at zero disparity. Evaluation of simultaneously recorded tuning profiles indicated the absence of detectable vergence movements between trials. Comparison of single and multiple units re-

The costs of publication of this article were defrayed in part by the payment of page charges. The article must therefore be hereby marked "*advertisement*" in accordance with 18 U.S.C. Section 1734 solely to indicate this fact.

corded at the same recording site revealed no convincing clustering of preferred disparities that may indicate a map of disparities.

METHODS

Behavioral protocol

Two tame barn owls (*Tyto alba*) from the institute's breeding stock were trained on a visual fixation task performed inside a sound-attenuated and darkened booth (Fig. 1). Birds rested on a perch 57 cm in front of a cathode-ray tube screen. Whenever the owl oriented its gaze toward the screen, a trial was automatically initiated and a fixation target was displayed. The fixation target consisted of two vertical black lines presented on a 1.5 × 1.5 deg white square. The two lines were 0.8 deg long, 0.1 deg wide, and separated by 0.2 deg. These dimensions of the fixation target were found to be the minimum size that could be detected reliably by well-trained and motivated animals. After a variable time delay (2–5 s), the fixation target turned zero degree for 400 ms on which the bird had to peck a key to get a reward. Correct responses were rewarded with a small piece of meat supplied from a feeder in front of the animals; in addition, a feeder light was turned on for 4 s. False alarms were "punished" with a warning sound. When the owls reached a high-performance rate, rewarding was gradually reduced to 70% of correct responses to elongate the daily training and recording session. After each correct response, however, the owls were reinforced by the feeder light. Well-trained owls performed a maximum of 200 trials per day, but typically about 150 trials per day.

Gaze orientation was detected automatically by means of an infrared reflex photoelectric device in combination with a light-reflexive foil attached at the top of the bird's head. A trial was interrupted whenever the birds made head movements larger than ±1.5 deg. During the training, owls learned to avoid head movements while fixating. Notable front-back variations in head positions were not observed, as owls resting on the fixed perch adopted very stereotyped fixation behavior. Lack of front-back head movements has also been confirmed in behavioral experiments where owls were supplied with a head-tracking device (van der Willigen, unpublished observation). Fixation was additionally controlled by observing the gaze and eyes under infrared illumination at high magnification on a TV monitor. Eye movements were not measured, but tuning curves were analyzed to confirm that data were not contaminated by vergence (see section *Influence of eye position*). Behavioral performance was controlled and monitored by custom-written software running on a Silicon Graphics workstation that also delivered the visual stimuli.

Preparation and recording in awake animals

After the owls performed this fixation task reliably for months, they were prepared for chronic recordings. The owls were given Valium (1 mg/kg) for sedation and were anesthetized with ketamine (15 mg · kg^{-1} · h^{-1}). After loss of reflexes, they were wrapped in a jacket and the head was fixed in an stereotaxic holder. The skin on the dorsal surface of the skull was opened along the skull's midline. A hole was drilled in the skull to expose the dura over one hemisphere. Stereotaxic coordinates were chosen to reach the region of the visuotopically organized forebrain representing the visual field adjacent to the area centralis (Pettigrew 1979). Three to four custom-built microdrives supplied with one or two microelectrodes were fixed to the skull with dental cement. High-impedance, platinum-blacked tungsten microelectrodes (10 MΩ, F. Haer & Co.) were used to record single units. They could be lowered several millimeters into the brain. Electrodes were aligned to penetrate the Wulst perpendicularly. Two tungsten wires inserted into the forebrain served as indifferent electrodes. To allow attachment of the spectacles with filter glasses needed for stereoscopic stimulation, both birds carried a metal bolt that had been fixed to the skull just above the beak. After implantation, the wound was suture-closed and treated with antibiotic ointment. Recordings started five or more days after surgery. Care and treatment of the owls were in accordance with the guidelines for

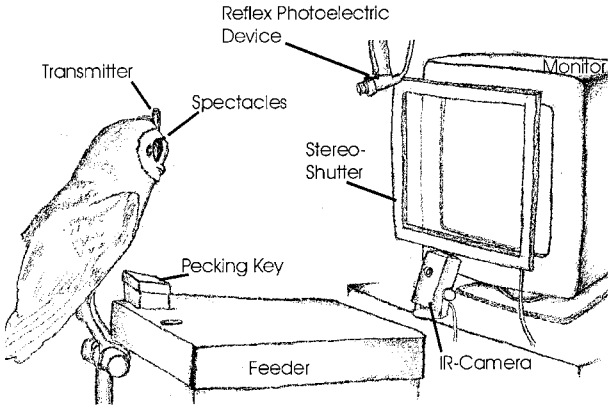

FIG. 1. Setup used for recording from behaving owls.

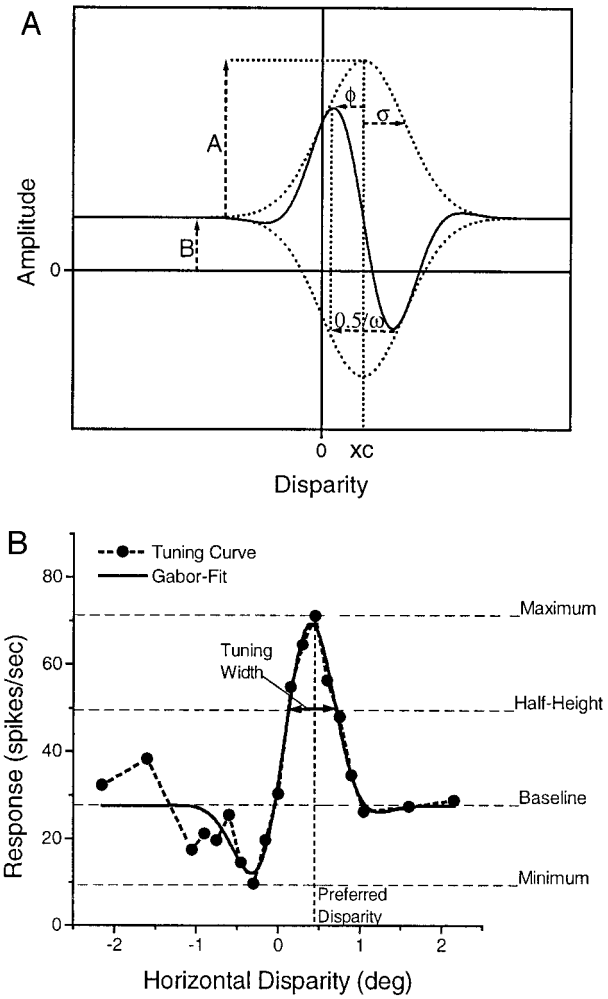

FIG. 2. Extraction of quantitative parameters by fitting a Gabor function to disparity-tuning curves. *A*: illustration of a Gabor function (solid line) and the 6 parameters that can be extracted when fitting the function to a measured disparity-tuning curve (see text for symbol explanation). The dotted envelope represents the Gaussian. *B*: a Gabor function was fitted to the profile and the offset was taken as a baseline. The tuning width was measured at half-height between maximum and baseline. The disparity that elicited a maximum discharge was termed "preferred disparity."

animal experimentation as approved by the Regierungs präsidium, Köln, Germany.

Extracellular unit recordings were performed primarily from the hyperstriatum accessorium of the visual Wulst. Neuronal signals were transmitted via radiotelemetry. The custom-built two-channel FM-stereo transmitter with a complementary metal oxide semiconductor (CMOS) high-impedance input stage weighed 6 g (including the batteries). The transmitter output was received by a dipole antenna and fed to a commercial FM-Tuner (Grundig Fine Arts), where the signal was demodulated. After filtering (band-pass 500-5000 Hz, cutoff 12 dB/octave) and amplification, the signals from both electrodes were monitored on a dual-channel oscilloscope and an audio monitor. Optimal tuning of the receiving system to the carrier frequency of the FM transmitter was checked continuously during the recording sessions. The recorded spike waveforms were digitized at a sampling rate of 32 kHz and stored on the disk of a PC equipped with a Datawave Discovery package. Preliminary cluster cutting was performed on-line to estimate the response characteristics during the on-going experiment. Final single-unit isolation was repeated off-line. All recordings analyzed contained only one or two well-separable single units.

Visual stimulation

Visual stimulation was performed by means of a Silicon Graphics Indy workstation running custom-written software incorporating OpenGL and GLUT graphics routines. The color monitor (Elsa 17H96, 16 in.) had a spatial resolution of 1280 × 1024 pixels and was refreshed at a frame rate of 76 Hz in mono mode (used for receptive field measurements). For stereoscopic presentations, graphics were switched to stereo mode with a spatial resolution of 1280 × 496 pixels and a refreshing rate of 120 Hz (60 frames per second for each eye). Stereoscopic presentation was accomplished by using a liquid crystal polarizer (NuVision SGS17S) that was placed in front of the display. The polarizer allowed alternate transmission of images for the left and right eye with circularly opposite light polarization in synchrony with the monitor's refreshing rate. In addition, the owls had to wear glasses filtering polarized light to allow the passage of the right eye's image to the right eye while blocking it for the left eye and vice versa. Interocular crosstalk was about 11% (white stimulus).

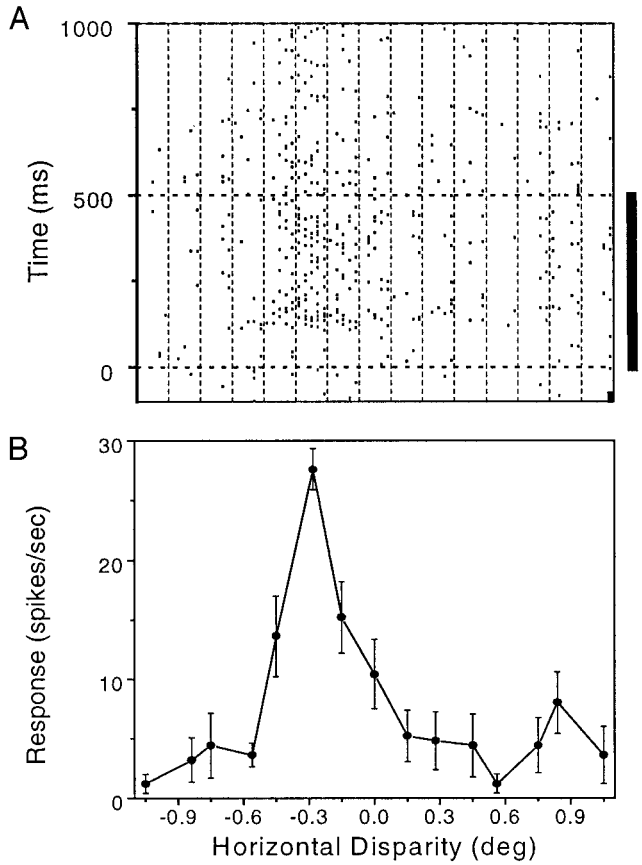

FIG. 3. Detailed illustration of a neuron's responses to random-dot stereograms with different horizontal disparities. *A*: dot-raster histogram. A sequence of pseudorandomized disparity values was repeated 5 times in this case. The occurrence of a spike is indicated by black dots. Horizontal grid lines separate different disparity values; vertical grid lines mark physical on- and offset of stimulus presentation (500-ms duration). *B*: disparity-tuning curve. The discharge of the neuron displayed in the dot-raster histogram was averaged over all stimulus repetitions per disparity value to construct a disparity-response profile. Error bars, SE.

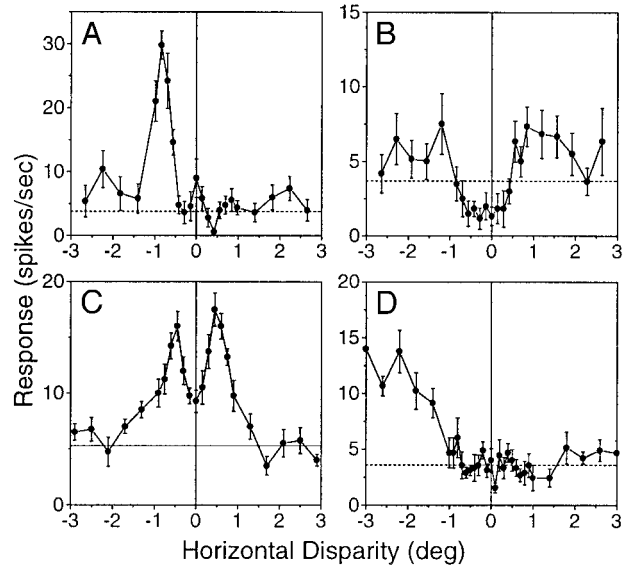

FIG. 4. Examples of disparity-tuning curves. The majority of neurons exhibited a single response peak (*A*). Response profiles with a prominent response dip (*B*) or 2 response peaks (*C*) were less frequent. Very few cells displayed an open-ended tuning curve (*D*).

Prior to stereoscopic stimulation, a neuron's receptive field (RF) was mapped with moving bars. The RFs (size ranging from 0.5 to 5 deg) were centered around the fixation target and did not exceed the stimulation area defined by the monitor screen.

To construct disparity-response profiles, static RDS covering the entire screen of the monitor around the fixation target were flashed for 500 ms on a black background. Therefore the stereogram completely covered the entire RF of the recorded units. Interstimulus interval was at least 1 s. The RDS consisted of 10% white and 90% black dots. The size of the rectangular dots was 0.15 deg. By shifting one of the two RDS images horizontally, positive or negative disparities could be introduced and the RDS appeared to float behind or in front of the fixation target that was always set to zero disparity as a reference. After each stimulus presentation, a new dot pattern was presented. A sequence of 19–23 different disparity values was presented. Disparity values were centered symmetrically around zero disparity in the range of ±2.15 to ±2.9 deg. The disparity range between ±0.9 deg was scanned in steps of 0.15 deg; disparity steps above 1 deg and below −1 deg, respectively, were larger. The sequence of disparities was pseudorandomized and repeated 5–15 times.

Data analysis

To construct a disparity tuning curve, the discharge rate was measured in a 500-ms time-window (according to the stimulus' duration) that was shifted by 60 ms relative to the physical stimulus onset to account for response latency. Disparity selectivity was statistically

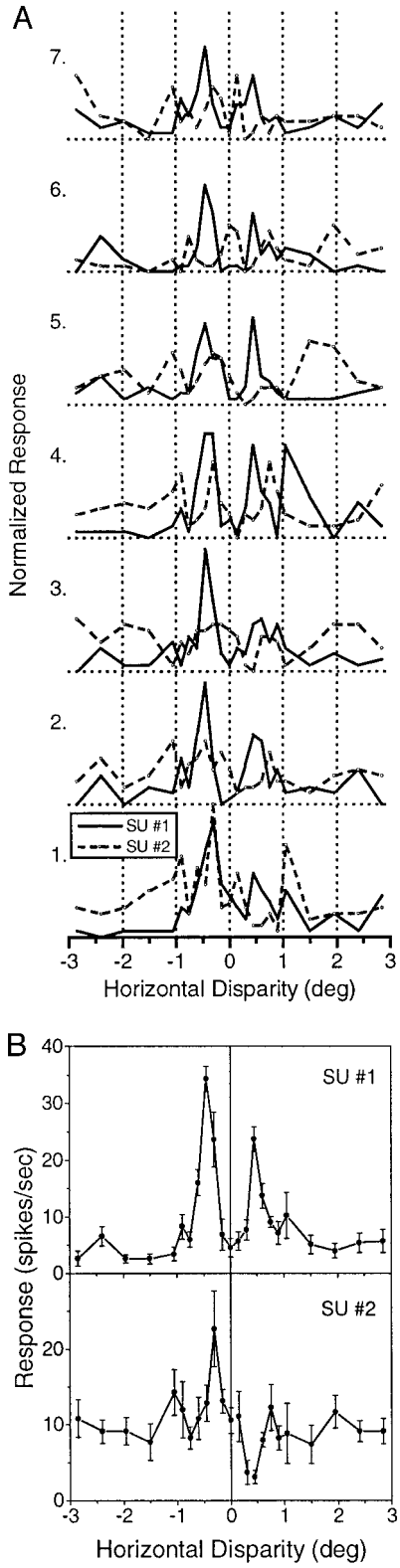

FIG. 5. Disparity tuning of 2 units simultaneously recorded at one electrode. *A*: single-trial tuning curves derived from 7 repetitions (*bottom to top*) of a pseudorandomized sequence of disparity values. *B*: tuning curves for both units derived from averaged discharge of all 7 trials displayed in (*A*). Note that the peaks of *unit 1* are not correlated to the discharge of *unit 2*, thus excluding external artifacts that would have affected both cells.

determined by calculating a nonparametric analysis of variance (ANOVA; Kruskal-Wallis *H*-test; criterion: $P < 0.05$, two-tailed). Spontaneous activity was derived from 100-ms intervals preceding stimulus onset, i.e., during presentation of a black screen without dots.

To derive quantitative measures, a Gabor function (Gabor 1946; Sanger 1988) was fitted to the response profiles derived from the mean firing rates as a function of disparity [$f(d)$]

$$f(d) = A * e^{-0.5[(d-xc)/\sigma]^2} * \cos(2\pi(\omega(d - xc) + \phi)) + B \qquad (1)$$

where A and B are the amplitude of the envelope and the firing rate offset (baseline), xc and σ are the position offset and the standard deviation of the Gaussian, and ω and ϕ are the frequency and phase of the cosine (Fig. 2*A*).

The fitting procedure was performed by using a Levenberg-Marquardt algorithm (χ^2 minimization). The fitting progression was graphically monitored after initial setting of suitable parameters. The baseline firing rate (B) of the fit was taken as a point of reference to measure the tuning profiles (Fig. 2*B*). In single-peaked response profiles, the tuning curve displayed only a single peak crossing the half-height line and, in addition, the response decreased to half-height on both sides of the peak. The disparity value that evoked the largest response for a given single-peaked cell was the "preferred disparity." The "disparity tuning width" of single-peaked cells was the continuous range of disparity values that excited the neuron at half-height level (see Fig. 2*B*). In cells that showed a larger amount of suppression (dip of the curve) than excitation (peak of the curve), or cells with two or more peaks crossing the half-height line, neither tuning width nor preferred disparity was measured.

The tuning index (TI) of a tuning curve was determined by

$$\mathrm{TI} = \frac{(R_{\max} - R_{\min})}{(R_{\min} + R_{\max})} \qquad (2)$$

where $R_{\max}$ and $R_{\min}$ are the maximum and minimum spike rate.

To compare disparity tuning profiles, the spike rate of *unit 1* at a given disparity was plotted against the spike rate of *unit 2* at the same disparity. Thus the relationship between both tuning curves could be studied with a simple regression technique

$$y = a + b * x \qquad (3)$$

where y is the spike rate of *unit 1* at a particular disparity, x is the response of *unit 2* at the same disparity, a is the intercept, and b is the slope of the x–y relationship. The comparison of disparity response profiles was performed statistically with a linear correlation analysis after Pearson ($P < 0.05$, two-tailed). If both tuning curves displayed identical profiles, data points of the resulting scatter plot lie on a straight line and the correlation coefficient is 1. A negative correlation was detected for profiles that were shifted by half a cycle.

RESULTS

According to the statistical criterion described above, 76% (122/160) of all investigated cells in the owl visual forebrain were found to be disparity selective. The proportion of disparity-selective cells was almost equal in both animals. In owl *Ki*, 80% of the units (69/86) displayed disparity sensitivity, whereas 72% of the cells (53/74) were disparity selective in owl *To*. A detailed illustration of the responses of a neuron to various disparities is presented in Fig. 3. This neuron was stimulated with five repetitions of a pseudorandomized sequence of different disparity values. It responded reliably to a preferred disparity of −0.3 deg and had a tuning width of 0.27 deg.

A correlation was found between the cells' spontaneous activity and disparity sensitivity. The mean spontaneous activ-

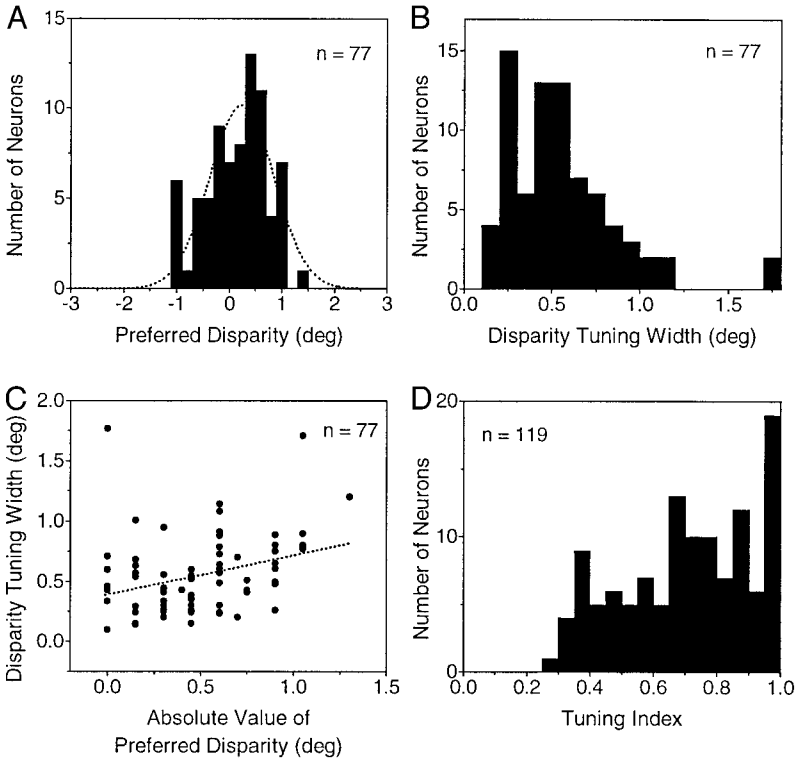

FIG. 6. Quantitative parameters derived from disparity-tuning curves. *A*: preferred disparities were distributed around zero degree (indicated by the Gauss fit). *B*: distribution of the curves' tuning widths. *C*: tuning curves became broader with increasing absolute values of preferred disparities. *D*: tuning index of all disparity-sensitive neurons.

ity of 3.7 spikes/s for disparity-sensitive units was significantly lower than the mean background activity of 7.6 spikes/s measured in disparity-insensitive neurons ($P = 0.009$, Mann-Whitney *U* test, two-tailed).

Response profiles

Tuning curves displayed a continuum of different shapes rather than discrete categories. Although some disparity-response profiles of cells in the behaving barn owl's visual forebrain resembled those described by Poggio and co-workers for cells in the visual cortex of the behaving primate (Poggio and Fischer 1977; for a review see Poggio 1995), there was a gradual transition between traditional response categories. Most neurons showed conspicuous damped periodic modulation. Indeed, Gabor functions that were suggested by models of disparity detection (for a review see Ohzawa 1998) provided reasonable fits to the tuning data (see Fig. 7).

Objective criteria (see METHODS) were applied to choose tuning profiles that exhibited only one dominant response peak and, hence, allowed the tuning width and preferred disparity to be measured. These single-peaked tuning curves (Fig. 4*A*) represented 63% (77/122) of all disparity-tuned cells. Several cells (12% of the total sample) experienced stronger suppression than excitation (with respect to baseline activity derived from a Gabor fit) within a certain range of disparities (Fig. 4*B*). The prominent dip of these suppressed cells was often flanked by mild excitatory peaks on both sides. Twenty-three percent of all neurons (28/122) were characterized by two, or rarely, three response peaks. Most of the double-peaked cells had maxima that were markedly symmetrically centered around the zero-degree axis (Fig. 4*C*). These cells typically exhibited activity at zero degree comparable to the discharge evoked by nonpreferred disparities. Two percent (3/122) of the neurons showed open-ended profiles, because activity increased up to the largest measured negative or positive disparity, without a defined peak (Fig. 4*D*). The proportion of different tuning profiles was about equal in both owls.

In Fig. 5, the responses of a single-peaked and a double-peaked neuron that were recorded simultaneously at one electrode are illustrated in detail. Single-trial tuning curves of each neuron are plotted in Fig. 5*A*. The pseudorandomized disparity sequence was presented seven times (from bottom to top). Although *single-unit 1* (double-peaked) showed prominent peaks at ± 0.45 deg for every single trial, *neuron 2* (single-peaked), which responded somewhat noisier, displayed a peak activity at -0.3 deg, but experienced substantial suppression of discharge at disparities around $+0.45$ deg. Comparing the averaged disparity-tuning curves (Fig. 5*B*) of both units indicates that the divergent tuning characteristics of these simultaneously recorded cells cannot be explained by external artifacts that would have affected both neurons' tuning. Most importantly, artifacts like variable eye movements cannot account for the double peaks of *unit 1*, because in this case also *unit 2* should have been excited (and not suppressed) at a disparity of about $+0.45$ deg.

Quantitative analysis

Preferred disparities of all 77 single-peaked neurons in both owls (Fig. 6*A*) clustered around zero degree (normal distribution, $P = 0.48$, one-sample Kolmogorov-Smirnov test). The mean preferred disparity for the entire sample of neurons was 0.12 deg. The range of preferred disparities was restricted (with one exception) to ± 1.1 deg.

The mean width of the disparity tuning curves measured at half-height between baseline activity and maximum amplitude of the curve was 0.55 deg (± 0.32 SD) (Fig. 6*B*). The width of

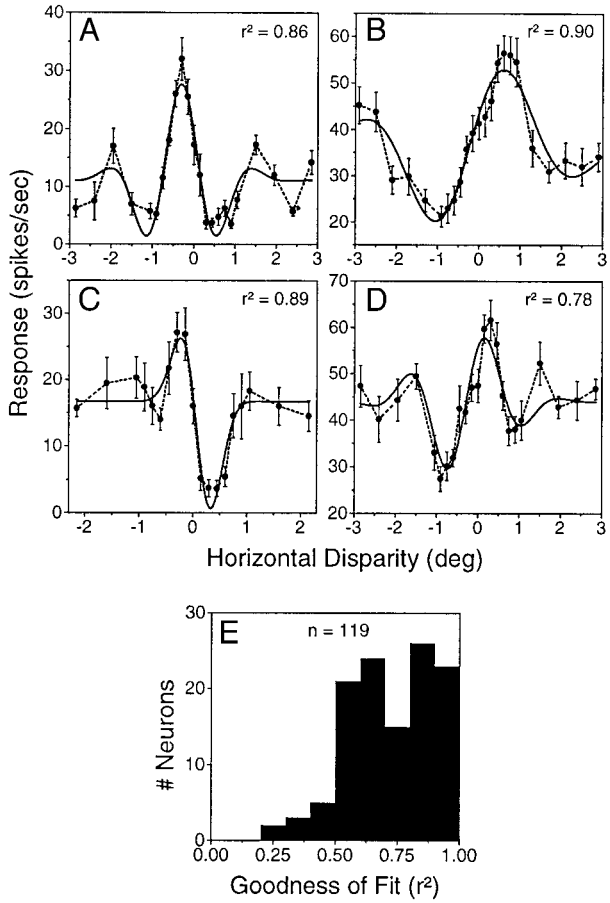

FIG. 7. Description of tuning profiles by Gabor function. *A–D*: Gabor function fitted to four disparity-response profiles. Dotted lines, neuronal data; solid lines, best fit. Goodness of fit (r^2) for individual profiles is given at the top of each panel. *A*: even-symmetric function. *B–D*: odd-symmetric functions. *E*: distribution of goodness of fit (r^2) for all fitted cells.

the tuning curves enlarged significantly with an increase of the preferred absolute value of disparity ($r = 0.32$, Spearman rank correlation coefficient, $P = 0.004$, $n = 77$, two-tailed). On average, the tuning width increased by 0.33 deg each degree of preferred disparity (Fig. 6*C*). The mean tuning index (Fig. 6*D*) in the awake owl was 0.71 (±0.21 SD).

To characterize tuning curves more quantitatively, several parameters derived from the Gabor fits were extracted. The disparity response profile of a disparity-energy detector is a Gabor function because it is based on Gabor subunits (Fleet et al. 1996; Ohzawa 1998; Ohzawa et al. 1990, 1997; Qian 1994; Zhu and Qian 1996). The implementation of the disparity energy model has not been shown directly in the owl, but the Gabor function provided reasonable fits for the majority of neurons in the visual Wulst (Fig. 7, *A–D*). For all 119 fitted tuning profiles (open-ended profiles were excluded), the goodness of fit (r^2) was, on average, 0.72 (±0.18 SD). In other words, 72% of the data can be explained by the fit. The distribution of the goodness-of-fit (Fig. 7*E*) demonstrates that the Gabor function provided a satisfactory description for most neurons.

The distribution of the envelope's position (position of the Gaussian) was centered around zero degree (mean: 0.04 deg ± 0.69 SD) (Fig. 8*A*) and resembled the distribution of preferred disparities (see Fig. 6*A*). The Gabor fits' width (Fig. 8*B*) (characterized by "sigma," σ, the standard deviation of a Gaussian) was, on average, 1.00 deg. The frequency ω of the cosine (Fig. 8*C*), the disparity frequency, exhibited a mean value of 0.44 cycles/deg (±0.31 SD). The disparity frequency of all single-peaked tuning curves was negatively correlated with increasing absolute values of preferred disparities ($r = -0.36$, $P = 0.003$, two-tailed, $n = 77$), suggesting sharper tuning around zero degree of disparity. The cosine's phase (Fig. 8*D*) was different from a uniform distribution ($P = 0.0073$, one-sample Kolmogorov-Smirnov test, $n = 119$).

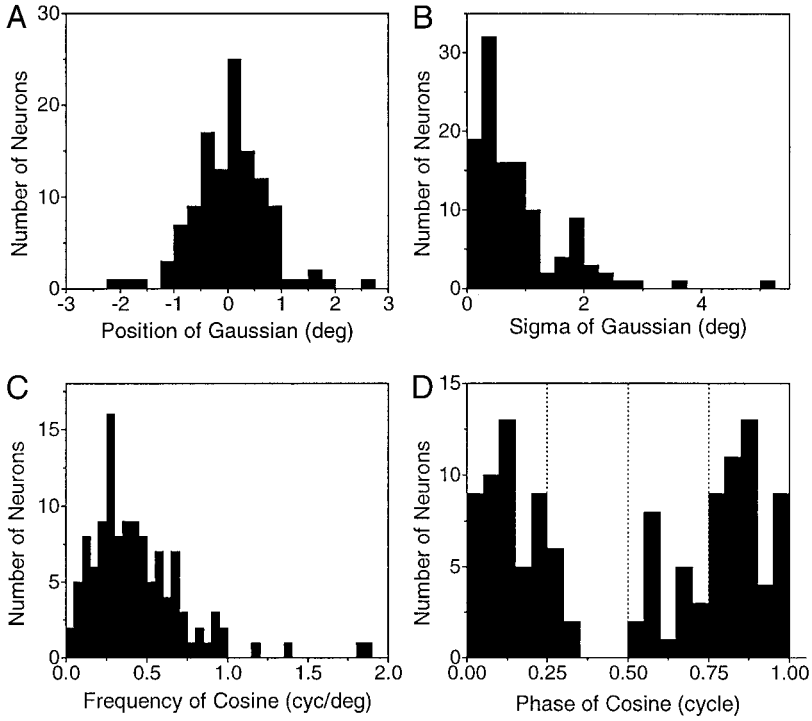

FIG. 8. Properties of disparity tuning curves derived from Gabor fits. Distribution of (*A*) position, (*B*) sigma, (*C*) disparity frequency, and (*D*) phase of the Gabor fits.

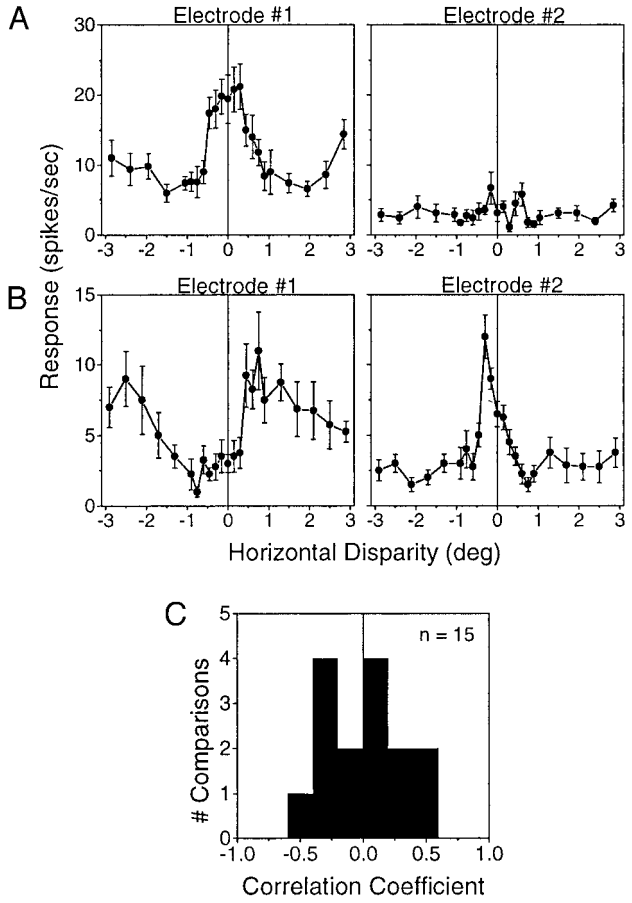

FIG. 9. Comparison of simultaneous recordings at different recording sites. *A*: single unit at *electrode 1* was significantly tuned to disparities around zero degree, whereas the neuron at the second recording sites was disparity insensitive ($P < 0.05$, *H*-test). *B*: both cells recorded simultaneously at different electrodes were tuned to certain disparities; however, the preferred disparities were quite different. *C*: distribution of correlation coefficients for all 15 cell pairs where both units were significantly tuned to disparity.

Phases around half a cycle were quite rare, whereas phases in the range of ± 0.25 were abundant.

Simultaneous recordings at two recording sites

Comparing the activity at two independent recording sites confirmed the assumption that the neurons per se were tuned to different disparities and that the preference for certain disparities was not an artifact caused by external factors. In 31 cases, responses of two single units were analyzed that were recorded simultaneously at two different electrodes spaced at least 1000 μm apart. In 15 comparisons (48%), both single units at two different electrodes were disparity sensitive. Tuning profiles recorded at different electrodes were compared with a correlation analysis after Pearson (see METHODS). In only one simultaneous recording, neurons at the different electrodes were significantly correlated, i.e., displayed similar tuning profiles. The remaining 14 recording pairs exhibited different tuning curves and preferred disparities (Fig. 9*B*). The mean correlation coefficient for all comparisons was 0.0 (± 0.30 SD) (Fig. 9*C*). In the remaining 16 comparisons (52%), only the neuron at one electrode was disparity sensitive, whereas the neuron at the other electrode was disparity insensitive (Fig. 9*A*).

Single units simultaneously isolated at the same recording site

In 20 recordings, two single units could be separated on the basis of their waveforms at an individual electrode tip. In three of the 20 recordings, both units were disparity insensitive. In four cases, only one of the two simultaneously recorded cells was disparity sensitive. For the remaining 13 recording sites at which both neurons were disparity selective, the disparity tuning profiles were compared with a correlation analysis. The tuning curves were significantly correlated (positively or negatively) in six cases. The profiles were anticorrelated (negative correlation coefficient) in two cases (15%), i.e., whenever one neuron got excited, the other cell became inhibited and vice versa (Fig. 10*A*). The correlation coefficient revealed a significant positive correlation for four cell pairs (31% of the sample where both units were disparity sensitive); in other words, both cells were excited or inhibited, respectively, at the same dis-

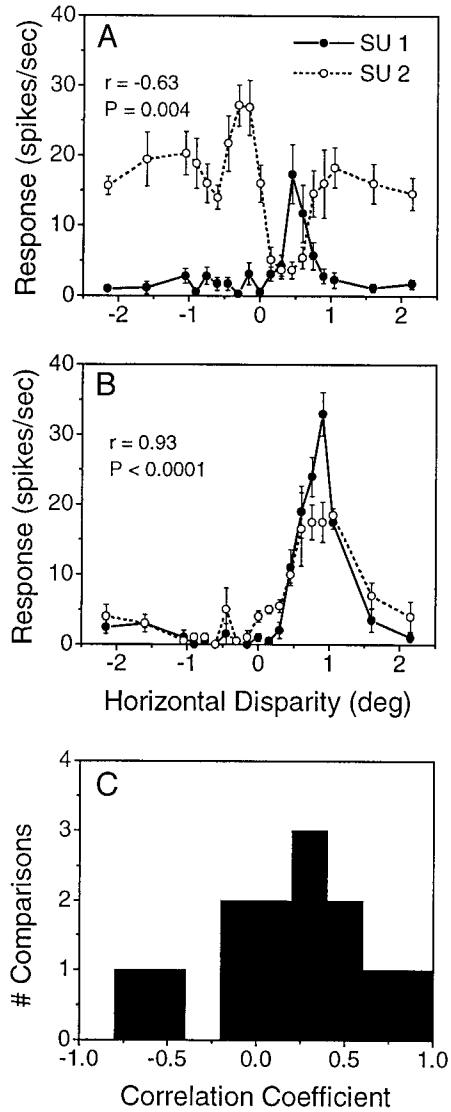

FIG. 10. Comparison of disparity response profiles of single units (SU) recorded simultaneously at identical recording sites. Pearsons correlation coefficient, *r*, and the significance level, *P*, is given for comparison of profiles. Examples where tuning curves were negatively correlated (*A*) or positively correlated (*B*). *C*: distribution of correlation coefficients for all single-unit comparisons.

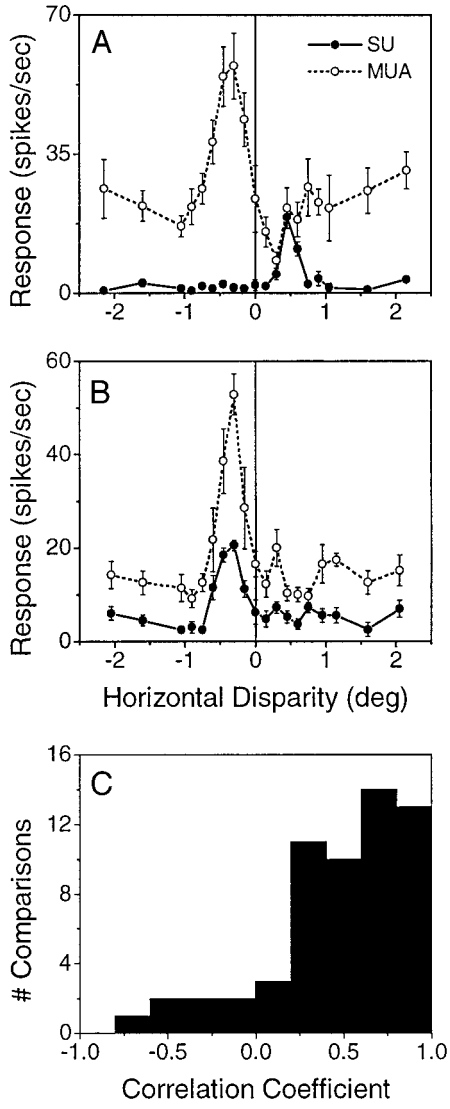

FIG. 11. Comparison of disparity-response profiles of single units (SU) and multiple-unit activity (MUA). Recording sites where tuning curves of SU and MUA were tuned to very different disparities (*A*) or almost identical (positive correlated) (*B*). *C*: distribution of correlation coefficients for all SU-MUA comparisons.

parity values (Fig. 10*B*). In seven cases (54%), the disparity profiles of neighboring units were not correlated; the disparity tuning differed from one another. The distribution of correlation coefficients is given in Fig. 10*C*.

Comparing single-unit and multiple-unit recordings

Single units (SU) and multiple-unit activity (MUA) was compared at 58 disparity-sensitive recording sites. Neuronal impulses were detected by means of a software level window discriminator. A MUA was defined as the number of all detected impulses subtracted by the well-isolated (waveform-separated) single-unit activity. To estimate the number of units in a cell cluster, the background activity of the MUA was divided by the single unit's spontaneous activity recorded at the same site. On average, the MUA consisted of 4.2 neurons. The disparity tuning of the MUA was not correlated to the tuning of the SU in 42% (24/58) of all cases (correlation analysis after Pearson, $P < 0.05$, two-tailed). In some cases, the SU and the MUA were sharply tuned to disparities of opposite sign (Fig. 11*A*). The tuning of both MUA and SU was positively correlated in 53% (31/58) of all observations. In these cases, the tuning profiles were almost identical (Fig. 11*B*). The remaining three recording sites (5%) exhibited a negative correlation between SU and MUA tuning; while the SU showed a response maximum, the MUA displayed a response minimum, and vice versa. Whether a SU and the corresponding MUA displayed correlated tuning profiles did not depend on the number of neurons per cluster ($P = 0.90$, Mann-Whitney *U* test, two-tailed). The distribution of correlation coefficients for all 58 comparisons is given in Fig. 11*C*.

Influence of eye position

Although eye movements are very restricted in owls (Knudsen 1982; Pettigrew and Konishi 1976; Steinbach and Money 1973), even small vergence variations could have considerable impact on disparity tuning. Thus we tested whether vergence eye movements might have had contaminated disparity tuning. Vergence movements during recording would shift tuning peaks and preferred disparity (Cumming and Parker 1999). To assess whether variable vergence influenced our data, we analyzed the variation of tuning peak position on a trial-by-trial basis for cases where two units (either SU or MUA) were recorded simultaneously and exhibited the same preferred disparity and tuning peak. In these cases, eye movements should shift the peaks of both tuning curves in the same direction (to more negative or positive disparities, respectively) for each disparity sequence. In other words, there should be a strong positive correlation (with unity slope) between the single-trial peak positions of *unit 1* and *unit 2*.

We fitted a Gauss function to single-trial tuning peaks of 28 pairs of simultaneously recorded units (6 pairs consisting of 2 single units and 22 pairs consisting of 1 SU and 1 MUA) that were tuned to the same preferred disparity. On average, a disparity sequence was repeated seven times in these cases. Fig. 12*A* shows typical single-trial tuning curves of one SU and one MUA recorded at the same electrode. The disparity sequence was presented seven times (from bottom to top); the top panel represents the standard averaged tuning curve. There was some variation in the discharges from trial to trial, but the slight jittering in the peak position of the optimal Gauss fits were not correlated between SU and MUA (Fig. 12*B*). The correlation coefficient of 0.12 at this recording site suggests that the slight jittering of the single-trial peaks was independent for both units. Figure 12, *C* and *D*, displays the unit pair that exhibited the most positive correlation ($r = 0.59$; $P = 0.16$) when comparing single-trial tuning peaks. The standard deviation of the peak jitter was 0.13 deg (SU) and 0.15 deg (MUA), respectively. On average, the mean correlation coefficient for all 28 analyzed pairs was normally distributed (KS test, $P = 0.49$) with a mean coefficient of 0.04 (Fig. 13). This suggests that vergence, if at all, had only a minor influence on the tuning profiles.

To obtain an estimate of the absolute peak jitter that occurred from trial to trial at individual units (either SU or MUA), the differences between all single-trial peak positions (derived from Gauss fits) were measured and pooled for all 56 units. The distribution of observed peak differences is summa-

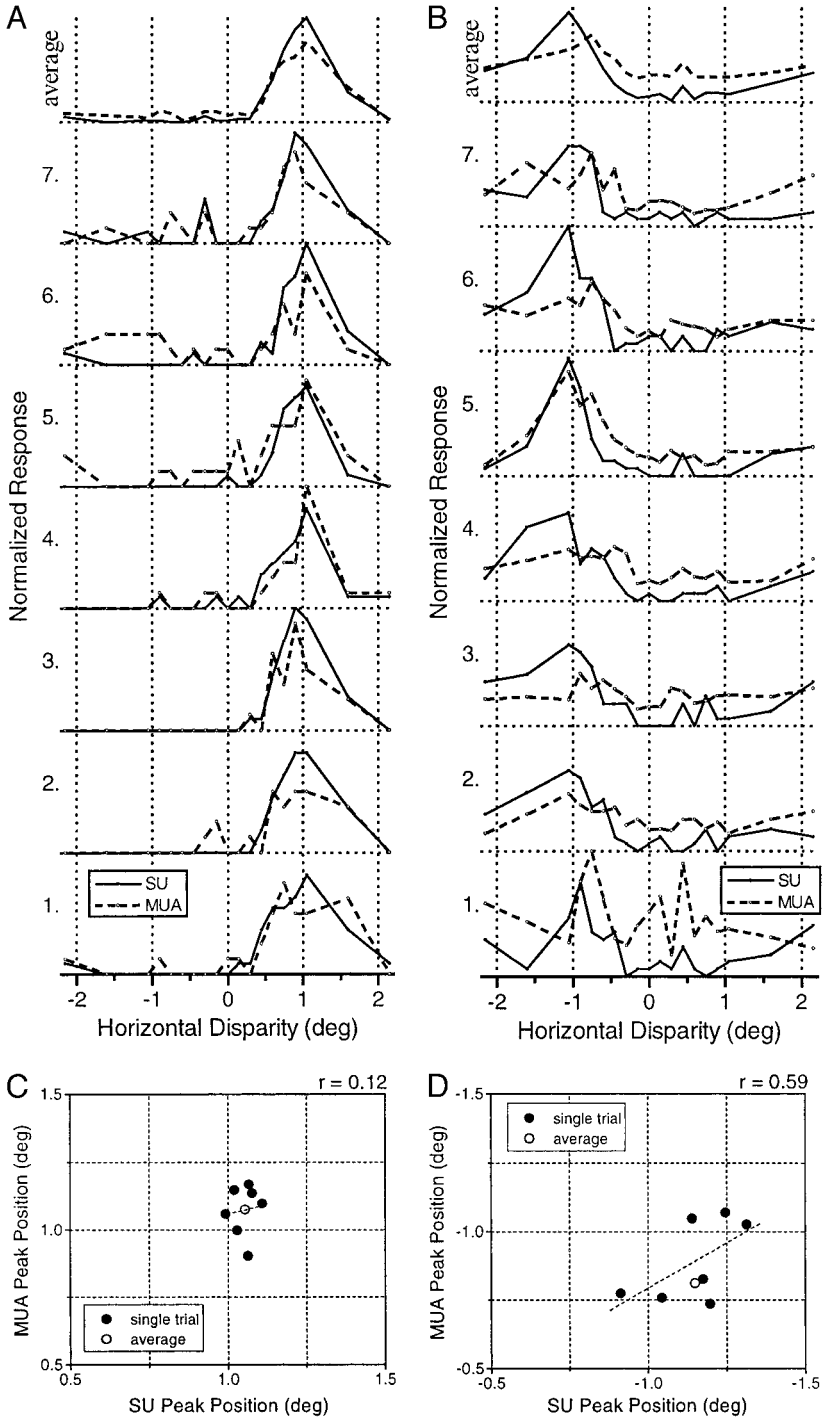

FIG. 12. Quantitative single-trial analysis of tuning of SU and MUA simultaneously recorded at the same recording site and tuned to identical disparity. *A*, *B*: recording site representing the condition found in most comparisons. *A*: disparity sequence was presented 7 times (*bottom to top*). Single-trial tuning curves were tuned at about 1 deg for both SU and MUA and result in the averaged tuning profiles displayed in the top panel. *B*: peak positions of the Gauss fit of the same recording site as in (*A*) for SU and MUA single trials plotted against each other. Correlation coefficient given at the top right corner. *C*, *D*: recording site that showed the most positive correlation for peak positions comparison of SU and MUA of all tested pairs. *C*: single-trial tuning curves for 7 representations of the disparity sequence. *D*: correlation between peak positions of SU and MUA of the same recording site as in (*C*).

rized in Fig. 14. The absolute jitter had a mean of 0.01 deg, and a standard deviation of 0.22 deg. This is much smaller than the mean tuning width of 0.55 deg. It is important to note that these position jittering was caused by all kinds of noise (see DISCUSSION).

Reproducibility of tuning over time

If disparity tuning found in visual neurons of behaving barn owls was an attribute of the neurons per se and independent of external factors, a given cell's tuning should be reproducible at different times. To confirm this requirement, the tuning profile derived for the first part of stimulus repetition was compared with the tuning curve for the second part of stimulus presentation for each individual neuron. Depending on the number of repetitions, temporal delay between the first and second part of measurement was in the range of 15–30 min. All neurons were compared with a correlation analysis if the total stimulus repetition was six or more (105 neurons of the 122 disparity-sensitive cells). For example, responses elicited during the first

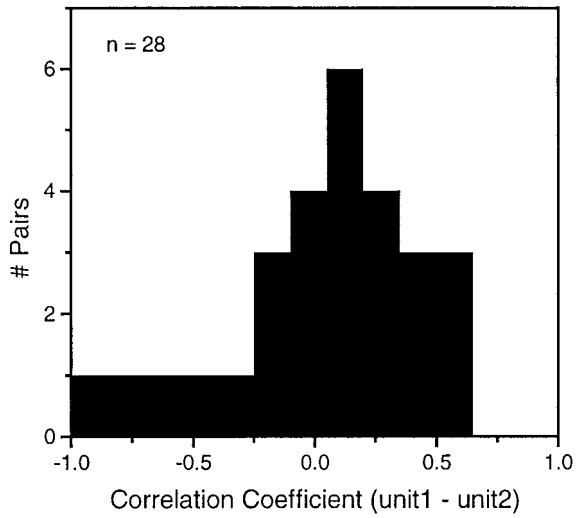

FIG. 13. Distribution of correlation coefficients for single-trial comparisons of peak positions for all 28 unit pairs. Correlation coefficients were distributed around 0.

three presentations were compared with activity evoked during the last three presentations for a neurons that was stimulated six times with the pseudorandomized sequence of disparities. Figure 15, *A–G*, displays examples of such split tuning curves for seven neurons. Tuning during the earlier stimulation period was almost identical to the tuning during the later period. This holds also true for cells with multipeaked profiles (Fig. 15, *E* and *F*), providing further evidence that response peak at more than one disparity value was not caused by artifacts such as variable eye alignment. Similarity of tuning profiles was confirmed by large correlation coefficients (mean $r = 0.65$) (Fig. 15*H*). In only 15% of the comparisons (16/105), correlation dropped below significance level ($r < 0.41$). As was the case for the single-trial comparisons performed in the section above, it is important to be aware of different noise sources inherent to recordings that might have caused variation in the tuning curves' shape.

DISCUSSION

The main result of this study is that neurons in the awake, fixating owl exhibit disparity sensitivity to global random-dot stereograms. Response curves could be fitted well with Gabor functions. Simultaneous single-unit recordings at different recording sites demonstrated that the neurons' tuning was independent and reliable across stimulus repetitions. Comparison of single units and multiple units at individual recording sites showed only very moderate clustering of preferred disparities. We shall discuss these findings in the following with respect to the literature on stereovision in mammals and owls.

Functional similarity of visual Wulst and mammalian visual cortex

In the current study, 76% of the neurons in the awake owl's visual Wulst responded to global stereoscopic stimuli. Compared to mammalian visual cortex, this represents a very high proportion. In V1 of the behaving monkey, 20–39% of the cells were found to be sensitive to disparities in RDS (Gonzalez et al. 1993; Poggio et al. 1985; 1988), whereas 29–57% of V2 neurons (Gonzalez et al. 1993; Poggio et al. 1985; 1988) and 50% of V3 neurons were disparity-sensitive (Poggio et al. 1988). Over 90% of the neurons in the medial superior temporal area (MST) display sensitivity to horizontal disparities when tested with moving RDS (Roy et al. 1992). Thus primate extrastriate visual areas tend to contain more neurons that are sensitive to global stereoscopic stimuli than striate cortex. From a functional point of view, the hyperstriatum accessorium of the visual Wulst resembles extrastriate cortical areas with regard to the proportion of disparity-sensitive neurons. This functional analogy is further supported by findings concerning proportions of preferred disparity. Although neurons in V1 were predominantly tuned at zero degree, tuned near and tuned far cells were the majority in V2 and V3 (Poggio et al. 1988). Neurons tuned at disparity other than zero degree were also the predominant types we found in the visual Wulst. Moreover, tuning width in the hyperstriatum accessorium seems to be comparable to extrastriate cortical areas like V2 (Burkhalter and van Essen 1986) and V3 (Fellemann and Van Essen 1987). Cells in more advanced areas tended to be more broadly tuned than those in the primary visual cortex (see Fig. 12 in Gonzalez and Perez 1998).

Double-peaked cells have not been described in awake monkeys so far. Double-peaked profiles are very likely not caused by variable vergence movements of the animals, because such an artifact should have had an impact on simultaneously-recorded units as shown in Fig. 5. Interestingly, many of those neurons had both peaks symmetrically centered around zero degree of disparity. Some of them would look very similar to TI cells for a restricted disparity range of about ± 0.5 deg (compare to TI cell of Fig. 13 in Poggio et al. 1988, where the cell was excited at ± 0.4 deg but responded with above spontaneous activity at 0 deg). We speculate that double-peaked tuning profiles are not special for owls, but may also be found in monkeys when testing disparities up to ± 3 deg.

Computational aspects of disparity detection

Many of the response profiles in the owl displayed prominent periodic modulation (see Fig. 7). This behavior of

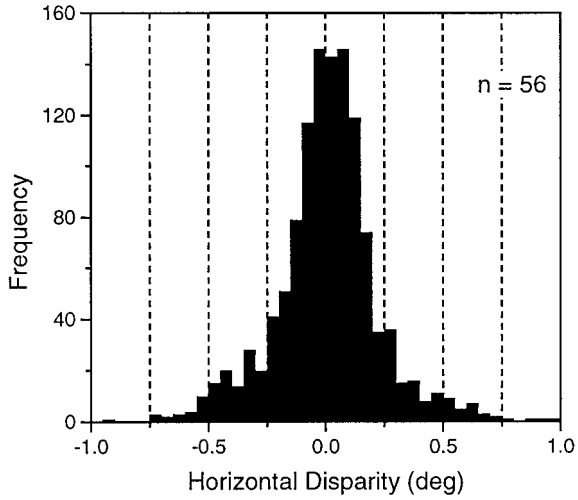

FIG. 14. Distribution of absolute peak jitter that occurred from trial to trial at all 56 analyzed individual units (either SU or MUA). Single-trial peak positions were derived from Gauss fits.

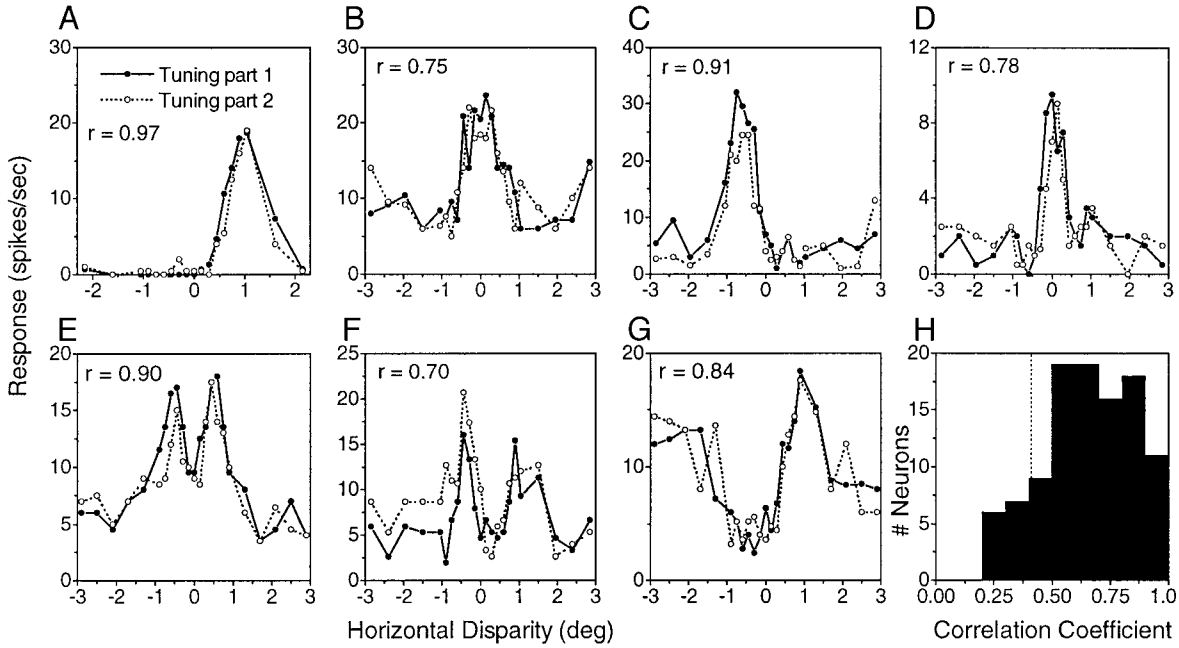

FIG. 15. Comparison of tuning curves derived during early (*part 1*) and late (*part 2*) period of stimulation. Examples of single-peaked (*A–D*), double peaked (*E–F*), and suppression-type (*G*) tuning profiles. Correlation coefficients *r* for pairwise curve comparisons are given in the left-hand corner. *H*: distribution of correlation coefficients for all 105 tested neurons. Vertical dotted line indicates significance threshold ($P = 0.05$).

disparity-sensitive neurons is expected for disparity detectors that are implemented according to the disparity energy model (Fleet et al. 1996; Ohzawa 1998; Ohzawa et al. 1990; Qian 1994; Zhu and Qian 1996). Because disparity energy neurons are based on subunits with Gabor-like spatial RF, the output of an ideal energy neuron can also be described by a Gabor function. Freeman and his collaborators (DeAngelis et al. 1991; Ohzawa et al. 1990, 1996, 1997) applied Gabor fits to describe disparity response profiles obtained with bar stimuli in the striate cortex of the anesthetized cat. Gabor functions provided also suitable fits for the majority of disparity tuning curves in the owl. This suggests that a similar algorithm to detect disparity information might be implemented in the avian forebrain.

The tuning profiles of most neurons in the owl can be explained by variation of model parameters (e.g., disparity frequency or phase of the cosine). Discrete classes of tuning types as proposed by Poggio and co-workers for cells in the awake monkey (Poggio and Fischer 1977; Poggio et al. 1985 1988) are questionable in the owl's forebrain when considering the distribution of neurons' tuning width. Although tuning width tended to be smaller around zero degree of disparity (see Fig. 6*C*), the scatter plot clearly shows a gradual transition to curves with larger/lower preferred disparities. Furthermore, the distinction between *tuned near/far* types and reciprocal types (*Near/Far*) strongly depends on the range of measured disparity in combination with the width of tuning (or the disparity frequency, respectively). With a measured disparity range of almost ± 3 deg, we only found three open-ended cells (of a total of 122 disparity-sensitive cells) that resembled *Near/Far* cells. If we would have had restricted the measured disparity range to ± 1 deg, many more open-ended profiles would have had occurred. A continuum of shapes has also been observed in mammalian cortex (Cumming and Parker 1999; DeAngelis and Newsome 1999; LeVay and Voigt 1988).

Clustered disparity representation?

The neural representation of sensory cues is often arranged in an orderly manner and may even form a sensory map. Clustering of cells preferring the same disparity has been described in the sheep's visual cortex (Clarke et al. 1976) and has recently been reported in monkey MT (DeAngelis et al. 1998; DeAngelis and Newsome 1999).

We therefore examined a putative clustered disparity representation in the awake owl by comparing *1*) single units that could be isolated at one electrode tip and *2*) multiple-unit activity and single-unit activity at individual recording sites. Instead of comparing adjacent neurons' preferred disparities alone (e.g., DeAngelis and Newsome 1999), a correlation analysis was used (see also Bradley and Andersen 1998) to account for the fact that many tuning curves were not characterized sufficiently by one dominant single peak. Many tuning profiles showed extensive periodic modulation or even more than one response peak.

The proportion of adjacent neurons tuned to similar disparities ranged from one-third (single-unit comparison) to one-half (single-unit versus multiple-unit activity). This suggests that few patches of identical disparity representation are present. Although an analysis of disparity tuning as a function of recording depth was not possible because high-impedance electrodes did not allow us to record single units in defined distances, it is, based on these findings, highly unlikely that the entire hyperstriatum accessorium is arranged in columns with identical disparity preferences or contains even a map of disparities. As a consequence, multiple-unit recordings in the owl's visual Wulst have to be interpreted with caution, because a mixture of response properties with respect to disparity coding is possible.

Evidence for fixation

Previous data on disparity tuning in the owl were collected in anesthetized animals (Pettigrew 1979; Pettigrew and Konishi 1976; Wagner and Frost 1993, 1994). Measuring disparity tuning curves in anesthetized preparations, however, bears several difficulties related to uncertainties about eye position and eye movements (for a detailed discussion see Orban 1991). In particular, estimating zero disparity is only possible in awake and fixating animals (Orban 1991).

We did not measure eye movements during awake recordings. How can we be confident that the owls fixated reliably at a given disparity? We trained owls in the awake preparation to focus on a fixation target as a plane of reference. By minimizing the fixation target so that it could just be reliably perceived by the owls, we forced the birds to fixate at zero degree of disparity. The distribution of preferred disparities as well as the distribution of the envelope of the Gabor fits almost precisely around zero degree of disparity strongly suggests that the owls really focused their view on the fixation target at zero degree. Because barn owls are able to exploit disparities around zero degree for stereoscopic depth vision (van der Willigen et al. 1998), the distribution of preferred disparities reported here emphasizes the behavioral relevance of disparity-sensitive neurons. Moreover, discharge to preferred disparities was reliable and statistically significant across stimulus repetitions (see Figs. 3 and 12). In addition, simultaneous single-unit recordings at different recording sites showed that the neurons' tuning was independent. In our opinion, the above-mentioned evidences confirm that the birds really fixated at the fixation target.

Vergence movements?

When recording disparity-tuning curves from an awake animal, the question arises whether the data are contaminated by vergence movements, a potential source of noise. The safest way to control vergence is to record movements of both eyes, a method usually adopted in studies with behaving monkeys where the head of the animal is fixed (e.g., Cumming and Parker 1999; DeAngelis and Newsome 1999). In the awake owl, however, we had to find other ways to record from birds performing a visual fixation task (Nieder and Wagner 1999), because motor responses used in behaving monkeys, like large eye movements or lever manipulation, cannot be exploited in owls. Instead, we trained the birds to use a pecking key to indicate changes of the fixation target, with the advantage of allowing a maximum of freedom to the birds during the task. As a consequence of this approach, the head of the owl had to be free, thus abolishing direct measurements of eye movements. Therefore we applied a post hoc analysis that allowed us to control whether vergence movements might have had influenced the disparity tuning data.

A correlation analysis of single-trial tuning curves of simultaneously recorded and identically tuned units allowed us to investigate systematic trial-to-trial variations that might had been caused by vergence. If an animal is forced to execute vergence movements during presentation of RDS, the disparity-tuning peak of a neuron shifts (Cumming and Parker 1999). In our study, the distribution of correlation coefficients did not reveal such a systematic influence. Nevertheless, we observed some jitter when comparing single-trial tuning peaks for several stimulus repetitions of individual units (Fig. 14). This jitter may be explained by at least two further sources of noise inevitably influencing neural responses. First, even if the stimulus is identical for several repetitions, the neural discharge shows some variance (*neural noise*); to overcome this problem, single-trial discharges are typically averaged. Second, random-dot patterns show local stimulus attributes (e.g., spatial frequency) that excite a neuron (that is locally restricted by its receptive field) better or worse (*stimulus noise*). Because the variations were not correlated in the two simultaneously recorded units, we conclude that vergence influenced our results much less than the other sources of noise inherent to electrophysiological recordings.

We thank R. van der Willigen and B. Gaese for programming support and M. Schäfer for help with data analysis. J. Lippert provided valuable comments on the data.

This work was supported by Deutsche Forschungsgemeinschaft Grant WA606/6 to H. Wagner.

Address for reprint requests: A. Nieder, Institut für Biologie II, RWTH Aachen, Kopernikusstr. 16, 52074 Aachen, Germany.

Received 22 October 1999; accepted in final form 1 February 2000.

REFERENCES

BOUGH, E. W. Stereoscopic vision in the macaque monkey: a behavioural demonstration. *Nature* 225: 42–44, 1970.

BRADLEY, D. C. AND ANDERSEN, R. A. Center-surround antagonism based on disparity in primate area MT. *J. Neurosci.* 18: 7552–7565, 1998.

BURKHALTER, A. AND VAN ESSEN, D. C. Processing of color, form and disparity information in visual areas VP and V2 of ventral extrastriate cortex in the macaque monkey. *J. Neurosci.* 6: 2327–2351, 1986.

CLARKE, P.G.H., DONALDSON, I.M.L., AND WHITTERIDGE, D. Binocular visual mechanisms in cortical areas I and II of the sheep. *J. Physiol. (Lond.)* 256: 509–526, 1976.

CUMMING, B. G. AND PARKER, A. J. Binocular neurons in V1 of awake monkeys are selective for absolute, not relative, disparity. *J. Neurosci.* 19: 5602–5618, 1999.

DEANGELIS, G. C., CUMMING, B. G., AND NEWSOME, W. T. Cortical area MT and the perception of stereoscopic depth. *Nature* 394: 677–680, 1998.

DEANGELIS, G. C. AND NEWSOME, W. T. Organization of disparity-selective neurons in macaque area MT. *J. Neurosci.* 19: 1398–1415, 1999.

DEANGELIS, G. C., OHZAWA, I., AND FREEMAN, R. D. Depth is encoded in the visual cortex by a specialized receptive field structure. *Nature* 352: 156–159, 1991.

FELLEMAN, D. J. AND VAN ESSEN, D. C. Receptive field properties of neurons in area V3 of macaque monkey extrastriate cortex. *J. Neurophysiol.* 52: 889–920, 1987.

FLEET, D. J., WAGNER, H., AND HEEGER, D. J. Neural encoding of binocular disparity: energy models, position shifts and phase shifts. *Vision Res.* 36: 1839–1857, 1996.

GABOR, D. Theory of communication. *J. Inst. Elec. Eng.* 93: 429–457, 1946.

GONZALEZ, F. AND PEREZ, R. Neural mechanisms underlying stereoscopic vision. *Prog. Neurobiol.* 55: 191–224, 1998.

GONZALEZ, R., KRAUSE, F., PEREZ, R., ALONSO, J. M., AND ACUNA, C. Binocular matching in monkey visual cortex: single cell responses to correlated and uncorrelated dynamic random dot stereograms. *Neuroscience* 52: 933–939, 1993.

JULESZ, B. Binocular depth perception of computer-generated patterns. *Bell System Tech. J.* 39: 1125–1162, 1960.

JULESZ, B. *Foundations of Cyclopean Perception*. Chicago: University of Chicago Press, 1971.

KARTEN, H. J., HODOS, W., NAUTA W.J.H., AND REVZIN, A. M. Neural connections of the "visual Wulst" of the avian telencephalon: experimental studies in the pigeon (*Columba livia*) and owl (*Speotyto cunicularia*). *J. Comp. Neurol.* 150: 253–278, 1973.

KNUDSEN, E. I. Auditory and visual maps of space in the optic tectum of the owl. *J. Neurosci.* 4: 1001–1011, 1982.

KNUDSEN, E. I. Fused binocular vision is required for development of proper eye alignment in barn owls. *Visual Neurosci.* 2: 35–40, 1989.

LEVAY, S. AND VOIGT, T. Ocular dominance and disparity coding in cat visual cortex. *Vis. Neurosci.* 1: 395–414, 1988.

NIEDER, A. AND WAGNER, H. Perception and neuronal coding of subjective contours in the owl. *Nature Neurosci.* 2: 660–663, 1999.

OHZAWA, I. Mechanisms of stereoscopic vision: the disparity energy model. *Curr. Opin. Neurobiol.* 8: 509–515, 1998.

OHZAWA, I., DEANGELIS, G. C., AND FREEMAN, R. D. Stereoscopic depth discrimination in the visual cortex: neurons ideally suited as disparity detectors. *Science* 249: 1037–1040, 1990.

OHZAWA, I., DEANGELIS, G. C., AND FREEMAN, R. D. Encoding of binocular disparity by simple cells in the cat's visual cortex. *J. Neurophysiol.* 75: 1779–1805, 1996.

OHZAWA, I., DEANGELIS, G. C., AND FREEMAN, R. D. Encoding of binocular disparity by complex cells in the cat's visual cortex. *J. Neurophysiol.* 77: 2879–2909, 1997.

ORBAN, G. A. Quantitative electrophysiology of visual cortical neurones. In: *Vision and Visual Dysfunction, Vol. 4: The Neural Basis of Visual Function*, edited by J. Cronly-Dillon. New York: MacMillan, 1991, p. 173–222.

PETTIGREW, J. D. Binocular visual processing in the owl's telencephalon. *Proc. R. Soc. Lond. B Biol. Sci.* 204: 435–454, 1979.

PETTIGREW, J. D. The evolution of binocular vision. In: *Visual Neuroscience*, edited by J. D. Pettigrew, K. J. Sanderson, W. R. Levick. Cambridge: Cambridge Univ. Press, 1986, p. 208–222.

PETTIGREW, J. D. AND KONISHI, M. Neurons selective for orientation and binocular disparity in the visual Wulst of the barn owl (*Tyto alba*). *Science* 193: 675–678, 1976.

POGGIO, G. F. Mechanisms of stereopsis in monkey visual cortex. *Cereb. Cortex* 3: 193–204, 1995.

POGGIO, G. F. AND FISCHER, B. Binocular interaction and depth sensitivity in striate and prestriate cortex of behaving rhesus monkey. *J. Neurophysiol.* 40: 1392–1405, 1977.

POGGIO, G. F., GONZALEZ, F., AND KRAUSE, F. Stereoscopic mechanisms in monkey visual cortex: binocular correlation and disparity selectivity. *J. Neurosci.* 8: 4531–4550, 1988.

POGGIO, G. F., MOTTER, B. C., SQUATRITO, S., AND TROTTER, Y. Responses of neurons in visual cortex (V1 and V2) of the alert macaque to dynamic random-dot stereograms. *Vision Res.* 25: 397–406, 1985.

QIAN, N. Computing stereo disparity and motion with known binocular cell properties. *Neural Comp.* 6: 390–404, 1994.

ROY, J.-P., KOMATSU, H., AND WURTZ, R. H. Disparity sensitivity of neurons in monkey extrastriate area MST. *J. Neurosci.* 12: 2478–2492, 1992.

SANGER, T. D. Stereo disparity computation using Gabor filters. *Biol. Cybern.* 59: 405–418, 1988.

STEINBACH, M. J. AND MONEY, K. E. Eye movements of the owl. *Vision Res.* 13: 889–891, 1973.

VAN DER WILLIGEN, R. F., FROST, B. J., AND WAGNER, H. Stereoscopic depth perception in the owl. *Neuroreport* 9: 1233–1237, 1998.

WAGNER, H. AND FROST, B. Disparity sensitive cells in the owl have a characteristic disparity. *Nature* 364: 796–798, 1993.

WAGNER, H. AND FROST, B. Binocular responses of neurons in the barn owl's visual Wulst. *J. Comp. Physiol. A Sens. Neural Behav. Physiol.* 174: 661–670, 1994.

ZHU, Y. AND QIAN, N. Binocular receptive field models, disparity tuning, and characteristic disparity. *Neural Comput.* 8: 1611–1641, 1996.